ARISTARCHUS CRATER AS A PROBE OF THE LUNAR CRUSTS MOST FRACTIONATED ROCK TYPES.

Michael Zanetti and Bradley L. Jolliff, Department of Earth & Planetary Sciences and the McDonnell Center for the Space Sciences, Washington University, Saint Louis, MO. michael.zanetti@wustl.edu

Introduction: Aristarchus Crater (~42 km diameter), located in the northwestern portion of Oceanus Procellarum on the southeastern boundary of the Aristarchus Plateau, has long been recognized for the unusual and diverse suite of materials it excavated [1-10]. Remote sensing data sets have provided increasingly more detailed and sharper focus on the characteristics of these materials. Most recently, LRO has obtained compositional data (Diviner, [11]) and high-resolution images (LROC-NAC [12]) that allow the correlation of compositionally distinctive signatures to specific morphological and lithologic units. From the integration of these data sets, we infer that the Aristarchus target section features a petrogenetically diverse suite of rocks including materials of the Aristarchus Plateau, young and relatively Th-rich basalts of Oceanus Procellarum, a differentiated, KREEP-rich igneous intrusive body, and diverse ejecta deposits from the Imbrium basin including olivine-rich materials [13] and KREEP-rich impact-melt deposits. Here we focus on the mapped distribution of these deposits, in particular, the compositionally evolved crustal materials.

Clementine data: The 1994 Clementine mission obtained multispectral data from which coupled mineralogy and compositional information were derived [5,6,7,14]. Plagioclase identifications and low FeO concentrations in the central peaks, derived from the UVVIS data indicated that the deepest materials excavated could be anorthositic [5,6,9,14]. According to these data, the crater interior and the brightest ejecta deposits have FeO concentrations of ~5-11 wt%.

Lunar Prospector: The 1998 Lunar Prospector Gamma-Ray Spectrometer (LP-GRS) results showed that Aristarchus Crater lies at the center of one of the strongest Th hot spots on the Moon [8,15,16]. Modeled values, taking into account the broad spatial response function, could be as high as 15 ppm [8]. Crater and proximal ejecta deposits, however, are lithologically mixed materials so some of the endmember rock components could have significantly higher concentrations. Using mixing trends, [17,18] argued that at least some of the materials excavated by Aristarchus are extraordinarily rich in Th, perhaps even more so than can be explained by a KREEP-rich substrate such as KREEP basalt (~13 ppm) or high-K Fra Mauro impact-melt breccia (~18 ppm). Lunar samples with the “right” Th and FeO values to satisfy mixing trends include Th-rich impact-melt breccia (Apollo 12, ~30 ppm Th [19], and potential differentiates of KREEP magmatism such as quartz-monzogabbro and granite.

Kaguya (Multiband Imager, Spectral Profiler) and Chandrayaan-1 (Moon Mineralogy Mapper): Multispectral and hyperspectral data for Aristarchus Crater have yielded higher quality spectral identifications of mineralogy, including both spectral and spatial resolution. The 2007 Kaguya (SELENE) mission multiband imager data indicate that Aristarchus central peak material may contain very pure crystalline anorthosite (PAN rocks with >98 vol %), and is the only location of these rocks within the Procellarum KREEP Terrane [20]. The interpretation of these rocks is based on the presence of a prominent 1.25 micron absorption band indicating a Fe-bearing crystalline plagioclase. The M3 hyperspectral imager on 2008’s Chandrayaan-1 mission, in contrast, revealed spectra of the central peak which are reported as very bright but lack any distinctive mafic or plagioclase absorption features, indicating that the central peak are dominated by low-Fe feldspathic materials [10]. Also identified in the ejecta of Aristarchus by both instruments are olivine dominated materials in the south and southeast portions crater walls and ejecta blanket [10,13,21], which can now be directly correlated photogeologically with specific surface features [e.g. 10,22].

LRO: The Diviner lunar radiometer includes three narrow spectral bands centered at 7.8, 8.25, and 8.55 μm that cover the Christiansen Feature (CF), which is sensitive to silicate mineralogy and the bulk SiO_2 content (essentially the degree of polymerization) [11]. On the basis of these data, ejecta on the southwestern rim of Aristarchus appear to be silicic, i.e., consistent with the presence of abundant quartz (or cristobalite or tridymite) and alkali feldspar, i.e., granite or alkali feldspar [11] (arrow in Fig. 1d). Narrow angle camera (NAC) images, with resolution of ~ 0.5 m/pixel, cover approximately 85% of the crater interior and the proximal ejecta blanket with variable illumination geometry. Detailed geomorphologic mapping of the crater is currently underway [22].

Discussion: Aristarchus Crater has an extensive bright ray system that extends several hundred km from the crater rim and these materials, along with rocks in the crater itself, constitute an unusual set of associations. In addition to basaltic components, the crater excavated very high albedo crater material and ejecta. High albedo materials are especially concentrated south and southwest of the crater rim (Fig. 1a), and olivine-rich rocks are concentrated in ejecta along a narrower radial deposit east – southeast of the crater [10]. This diversity of lithologic materials associated with the crater and located in the target area reflect the diversity of the target rock formations that exist in the upper few km in this region, and the specific target rocks may be highly localized. Furthermore, some of the components are not easily relatable to specific morphologic units [10,22] and cannot be explained by any simple petrogenetic scenario. For example, compositionally evolved KREEP-rich rocks and olivine-rich rocks [13] are not expected together, and we infer that these may simply reflect juxtaposition of Imbrium ejecta deposits with evolved intrusive rocks of the PKT. Possible origins of the olivine-rich material are discussed by [13]. The high albedo materials, including those within the crater and the SW ejecta unit are most likely low-FeO, alkali-rich differentiates of a KREEP-rich, near-surface intrusive body and not primary anorthosite of the Moon's early primary crust.

Given the extensive volcanic activity that occurred in this region of the Moon, basaltic underplating, as suggested by Hagerty et al. [23], of KREEP rich rocks, may have caused partial melting and intrusion of silicic magma (with a small degree of melting) or melting and injection of an evolved KREEP-rich magma such as quartz monzogabbro to a shallow level in the Aristarchus target section. Aristarchus occurs close to two other localities where evolved, silicic volcanics are indicated by compositional and morphological data, the Mairan and Gruithuisen Domes [8,11,23], which may indicate that this was a special or even unique petrologic province on the Moon.

Acknowledgements: We gratefully acknowledge the LRO Project and the LROC Team for their work in collecting the data and for support of this research.

References: [1] Guest (1973) GSA Bulletin 84. [2] Zisk et al. (1977) Moon 17. [3] Etchegaray-Ramirez et al. (1983). JGR 88 supplement p A529-A543 [4] Guest & Spudis (1985) Geol. Magazine 144. [5] Lucey et al. (1986) JGR 91. [6] McEwen et al. (1994) Science 266. [7] Le Mouélic et al. (1999) GRL 26. [8] Hagerty et al. (2009) JGR 114. [9] Chevrel et al. (2009) Icarus 199. [10] Mustard et al. (2011) JGR 116. [11] Glotch et al. (2010) Science 329. [12] Robinson et al. (2010) Space Science Reviews, 150. [13] Wiseman et al. (2012) LPSC 43, Abs #2515. [14] Pinet et al. (1999) LPSC 30, Abs 1555. [15] Lawrence, D. et al. (2003) JGR 108. [16] Lawrence, D. et al. (2007) GRL 34. [17] Jolliff (2004) LPSC 35, Abs #2032. [18] Zhang and Jolliff (2008) LPS 39, #2534. [19] Korotev et al. (2011). Geo Chem Acta 76, 6 [20] Ohtake et al (2009) Nature, 461. [21] Yamamoto et al., (2010) Nat Geo, 3. [22] Zanetti et al. (2011) LPSC 42, Abs #2330. [23] Hagerty et al., 2006 JGR 111. [24] Scholten F. et al. (2012) JGR 117, E00H17.

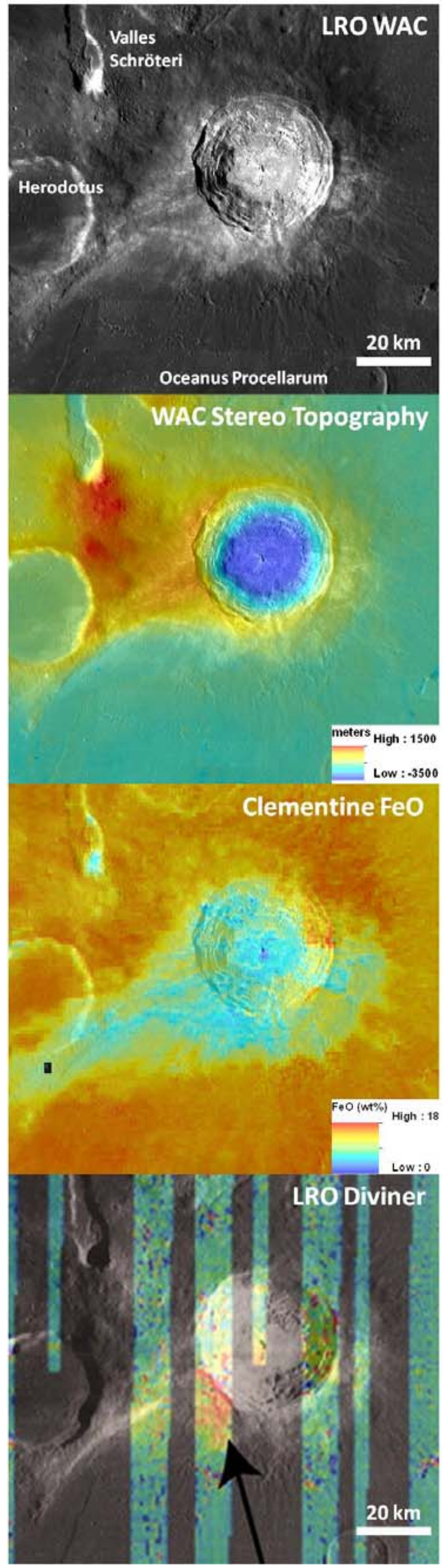

Figure 1: Aristarchus Crater situated on the SE edge of the Aristarchus Plateau. A) LRO WAC image, 100 mpp mosaic, B) WAC derived stereo topography, GLD100 [24], C) Clementine UV-VIS-derived FeO, D) LRO Diviner data (modified from [11]).